applied sciences

MDPI

Article

Comparative Thermal and Mechanical Characterization of MDF Panels Produced by Hot and Cold Pressing with Different Vertical Density Profiles

Szymon Kowaluk [1] and Grzegorz Kowaluk [2,*]

[1] Faculty of Information and Communication Technology, Wrocław University of Science and Technology, Janiszewskiego St. 11/17, 50-372 Wrocław, Poland; 284475@student.pwr.edu.pl
[2] Department of Technology and Entrepreneurship in Wood Industry, Institute of Wood Sciences and Furniture, Warsaw University of Life Sciences—SGGW, Nowoursynowska St. 159, 02-787 Warsaw, Poland
* Correspondence: grzegorz_kowaluk@sggw.edu.pl

Featured Application

The present study compares MDF panels manufactured using two different pressing routes, resulting in conventional U-shaped and approximately flat vertical density profiles. The hot-pressed panels exhibited higher thermal conductivity and bending performance, whereas the cold-pressed panels showed higher internal bond strength. These differences reflect the combined influence of manufacturing conditions and the resulting internal structure, including possible differences in fibre consolidation and adhesive curing. The findings provide preliminary information relevant to the development of MDF substrates for underfloor heating, although further investigations under controlled manufacturing and service conditions are required.

Abstract

The thermal performance of wood-based flooring over underfloor heating depends on panel density and through-thickness structure. This study compared medium-density fibreboard (MDF) panels manufactured by hot and cold pressing, resulting in conventional U-shaped and approximately flat vertical density profiles (VDPs), at nominal densities of 500, 600, and 700 kg m^{-3}. Thermal conductivity, thermal resistance, and heat flux were determined using two specimens per variant ($n = 2$), while mechanical properties were evaluated using specimens from three independently manufactured panels per variant. Corresponding U- and F-profile panels differed in mean density by only 0.6–2.0%, but exhibited markedly different thermal behaviour. Thermal conductivity was 0.0804, 0.1054, and 0.1199 W m^{-1} K^{-1} for the hot-pressed U500, U600, and U700 panels, respectively, compared with 0.0713, 0.0728, and 0.0885 W m^{-1} K^{-1} for the corresponding cold-pressed F500, F600, and F700 panels. Thus, the cold-pressed panels exhibited 11.3%, 31.0%, and 26.2% lower thermal conductivity, respectively, than their hot-pressed counterparts. Hot-pressed panels with U-shaped profiles exhibited higher modulus of rupture (MOR) and modulus of elasticity (MOE), whereas cold-pressed panels with approximately flat profiles showed higher internal bond strength (IB). Differences in compressive stress at 10% strain diminished at the highest density. These findings reflect the combined effects of manufacturing conditions and the resulting internal structure, rather than the isolated influence of VDP. The thermal comparisons are preliminary because only two specimens were investigated per variant.

Check for updates

Academic Editor: Constantinos A. Balaras

Received: 4 September 2026
Revised: 15 October 2026
Accepted: 19 October 2026
Published: 23 October 2026

Copyright: © 2026 by the authors. Licensee MDPI, Basel, Switzerland. This article is an open access article distributed under the terms and conditions of the Creative Commons Attribution (CC BY) license.

Keywords: wood-based panels; underfloor heating; thermal conductivity; thermal resistance; density profile; mechanical properties

1. Introduction

Radiant floor heating is increasingly used in energy-efficient buildings because it enables heat delivery over a large surface area at relatively low operating temperatures and can provide favourable thermal comfort compared with conventional point-source heating systems. The performance of such systems is, however, influenced not only by the heating installation itself but also by the thermal properties of the floor covering placed above it. In particular, the thermal conductivity and thermal resistance of the flooring affect the rate at which heat is transferred from the heating system to the indoor environment. Consequently, the selection and structural design of flooring materials are important components of the overall thermal performance of radiant floor systems [1,2]. Simulation studies have also demonstrated that the performance of wooden flooring cannot be described by a single universal thermal-resistance threshold, because the effects of flooring properties depend on building characteristics and climatic conditions [2,3].

Wood and wood-based materials present a particular challenge in this context. Their relatively low thermal conductivity is beneficial in conventional building-envelope applications but may restrict heat transfer when they are used directly above a heating system. Seo et al. [1], investigating different wood-flooring constructions, demonstrated that thermal performance depended strongly on the structure and composition of the flooring system. Laminate flooring exhibited comparatively favourable heat-transfer characteristics, which the authors associated with its relatively high density and thin constituent layers. The method of installation was also important, as additional air layers in floating systems reduced heat-transfer efficiency [1]. These observations indicate that optimization of wood flooring for radiant heating should consider not only the intrinsic properties of the constituent material but also its internal structure and the arrangement of solid and porous regions through the heat-flow direction. In addition to the intrinsic thermal conductivity of the material, effective heat transfer in layered systems may be influenced by interfacial thermal resistance and coupled heat and moisture transport. Previous investigations involving porous and multilayered materials have demonstrated the importance of thermal contact conditions and the limitations of simplified heat-transfer models [4]. Although these findings do not directly describe the behaviour of MDF panels, they provide useful methodological perspectives for interpreting thermal measurements and designing future experiments under transient conditions.

Medium- and high-density fibreboards are widely used as structural substrates in laminate and engineered flooring because they offer homogeneous in-plane structure, good machinability, dimensional accuracy, and mechanical properties that can be controlled through raw-material selection and pressing conditions. However, fibreboards are not structurally homogeneous through their thickness. Conventional hot pressing produces a characteristic VDP, generally characterized by highly densified outer layers and a lower-density central region. The development of this profile results from coupled heat and mass transfer, mat moisture distribution, press-closing strategy, material softening, and time-dependent consolidation during pressing [5,6]. Minhas et al. [5] demonstrated that pressing temperature, pressure, cycle time, and mat moisture content affect both peak and core densities of MDF and consequently influence its mechanical properties. Thus, VDP can be regarded as a macroscopic representation of the consolidation history and internal architecture of the panel rather than merely as a consequence of its mean density.

The mechanical consequences of VDP have been studied considerably more extensively than its thermal implications. The high-density outer regions of conventional fibreboard are particularly effective in bending because they are located far from the neutral axis, where tensile and compressive stresses reach their highest values. Previous studies have therefore shown that panels having similar mean densities may exhibit markedly different MOR and MOE depending on the distribution of density through the thickness [6,7]. Zhang and Yu [7], for example, demonstrated that redistribution of material towards the outer regions can substantially increase bending performance without increasing average panel density. Conversely, properties governed predominantly by the central region, particularly IB, are more closely associated with core density and the quality of bonding within this weakest zone. This means that increasing face density, core density, or mean density does not necessarily produce equivalent effects on different mechanical properties.

A comparable structural complexity can be expected for heat transport. Thermal conductivity of wood-based panels generally increases with density because increased compaction reduces air-filled porosity and increases the amount and connectivity of the solid lignocellulosic phase [8]. Nevertheless, bulk density alone does not fully characterize thermal transport in porous fibre-based composites. Fibre orientation, pore morphology, fibre-to-fibre contact area, moisture content, resin distribution, and the continuity of solid-phase conduction pathways may all contribute to effective thermal conductivity [8,9]. Measurements of wood-based panels have also demonstrated pronounced anisotropy of heat transport, confirming that the spatial organization of the material is relevant in addition to its overall density [8]. Recent investigations of wood-fibre boards further indicate that changes in fibre composition and consolidation conditions can simultaneously affect thermal conductivity and mechanical resistance, suggesting that both groups of properties may be linked to common features of the internal fibre network [10].

Despite these findings, the role of the through-thickness density distribution in controlling heat transfer through MDF remains insufficiently understood. Existing VDP research has predominantly addressed the effects of pressing parameters and density distribution on bending strength, stiffness, internal bonding, and related mechanical properties [5–7], whereas studies of wood flooring for radiant heating have mainly considered bulk thermal conductivity, total flooring thickness, material composition, and installation method [1–3]. Consequently, there is limited experimental evidence on whether two fibreboards of comparable mean density but fundamentally different vertical density profiles also differ in through-thickness thermal conductivity and thermal resistance. Even less information is available on how such differences interact simultaneously with bending performance, internal bond strength, and compression perpendicular to the panel plane. This distinction is important because optimizing a panel solely for thermal conductivity may compromise properties governed by different regions of its cross-section, while increasing mean density to improve heat transfer increases material consumption and may not represent the most efficient structural solution.

The concept of density-profile engineering therefore offers an alternative approach. Instead of changing only the total amount of material per unit volume, the fibre mass can be spatially redistributed through the panel thickness to modify the relative contribution of surface and core regions. For flooring applications, such an approach could potentially provide high-density outer regions promoting heat transfer and bending performance while retaining sufficient core consolidation to ensure internal cohesion and resistance to through-thickness loading. The resulting optimization problem is inherently multi-objective and requires simultaneous consideration of thermal and mechanical responses.

The aim of this study was to compare the thermal and mechanical properties of MDF panels manufactured using two distinct pressing routes, resulting in conventional U-shaped

and approximately flat vertical density profiles. Panels were produced at three nominal density levels (500, 600, and 700 kg m^{-3}), and their through-thickness density distribution, thermal conductivity, thermal resistance, bending properties, internal bond strength, and compression perpendicular to the panel plane were investigated. The study was intended to identify differences associated with the resulting manufacturing-induced internal structures rather than to isolate the causal effect of VDP. Although the investigated panels may be relevant to flooring applications over radiant heating systems, the present study was limited to the characterization of individual MDF specimens and did not evaluate the transient or steady-state performance of a complete flooring assembly.

2. Materials and Methods

2.1. MDF Panel Manufacturing

Laboratory MDF panels were manufactured from industrial pine (*Pinus sylvestris* L.) and spruce (*Picea abies* (L.) H. Karst.) fibres dried to a moisture content of approximately 4%. The fibres were bonded with a self-curing powdered urea-formaldehyde adhesive UF 68.02 PD (Zeno Line, CDW Sp. z o.o., Psary Małe, Poland) at an adhesive content of 12% based on the oven-dry mass of fibres. The adhesive was prepared according to the manufacturer's instructions by mixing two parts by weight of adhesive powder with one part of room-temperature demineralised water until a homogeneous mixture was obtained.

The resinated fibres were manually formed into 320 mm × 320 mm mats and pressed to a nominal thickness of 10 mm and nominal densities of 500, 600, and 700 kg m^{-3}. Two distinct pressing procedures were investigated, each producing panels with a characteristic vertical density profile. The U-profile panels were hot-pressed at 180 °C under a maximum unit pressure of 2.5 MPa, using a press factor of 20 s mm^{-1} of nominal panel thickness, corresponding to a total pressing time of 200 s. The F-profile panels were cold-pressed at 20 °C under a unit pressure of 1.2 MPa for 5 h. The resulting panels were designated U500, U600, U700, F500, F600, and F700, where the letter indicates the VDP type and the number indicates the nominal panel density in kg m^{-3}. For each panel variant, three independent panels were manufactured in separate pressing runs, resulting in a total of 18 panels. Each panel represented an independent manufacturing replicate. For each mechanical property, five specimens were obtained from each panel, resulting in 15 specimens per variant. Specimens originating from the same panel were considered subsamples rather than independent manufacturing replicates.

After pressing, the panels were conditioned under 20 ± 1 °C and 65 ± 1% RH until constant mass was reached. Although the panels were conditioned under controlled temperature and relative humidity, the actual moisture content of the specimens at the time of thermal testing was not independently quantified. This limits the assessment of the possible contribution of moisture-related differences to the measured thermal properties.

2.2. Specimen Testing

The MOR and MOE were determined by three-point bending in accordance with EN 310:1993 [11]. Internal bond strength (IB), expressed as tensile strength perpendicular to the plane of the panel, was determined according to EN 319:1993 [12]. Compressive stress at 10% strain (σ_{10}) was determined perpendicular to the panel plane according to EN ISO 29469:2022 [13]. All mechanical tests, if not described above, were performed following the specimen preparation, testing geometry, loading configuration, and test-rate requirements specified in the respective standards. No intentional deviations from the standardized testing procedures were introduced. A detailed spatial sampling map was not available; therefore, potential within-panel positional effects could not be evaluated separately. Fifteen specimens were tested per panel variant and mechanical property. For the mechanical tests,

a custom-built laboratory testing machine developed by the Research and Development Centre for Wood-Based Panels Sp. z o.o. (Czarna Woda, Poland) was used. In addition, the through-thickness density distribution of the manufactured panels was characterized using specimens with nominal dimensions of 50 mm × 50 mm × panel thickness. Density profiles were obtained by direct X-ray densitometry using a Grecon DA-X system (Fagus-GreCon Greten GmbH & Co. KG, Alfeld, Germany), with measurements recorded at a scanning resolution of 0.02 mm through the panel thickness. The surface and core density values were determined directly from the measured vertical density profiles. For each profile, the local density maxima occurring near the two panel surfaces were identified, and their arithmetic mean was used as the surface density descriptor. The core density was determined as the local density minimum within the central region of the panel thickness. The surface-to-core density ratio was subsequently calculated from these values. The coefficient of variation of the vertical density profile was calculated as the standard deviation of local density measurements divided by their arithmetic mean and expressed as a percentage. Thus, the reported surface and core density parameters represent characteristic local density values rather than average densities calculated over predefined layer thicknesses. Consequently, no fixed thickness boundaries between the face and core regions were required.

2.3. Thermal Measurement Procedure and Quality Control

The thermal measurements were performed in accordance with EN 12664:2002 [14] using a NETZSCH HFM 446 Lambda M heat flow meter (NETZSCH-Gerätebau GmbH, Selb, Germany) on samples measuring 300 mm × 300 mm. According to the manufacturer's documentation, the instrument employs a calibration procedure based on certified reference materials of known thermal conductivity, including NIST SRM 1450d fibrous-glass board (nominal thickness approximately 25 mm). Alternative reference materials include IRMM-440 and its successor, ERM-FC440. The MDF specimens were positioned horizontally between two temperature-controlled plates, with their principal surfaces facing the plates and heat flow directed perpendicular to the panel plane. Measurements were performed at a mean specimen temperature of approximately 10 °C, with a temperature difference of 18 K and a contact pressure of approximately 2 kPa. The selected mean temperature of approximately 10 °C provided a common laboratory condition for comparing the six panel variants. It was not intended to reproduce the full range of temperatures encountered during underfloor-heating operation. Thermal equilibrium was determined using the user-defined stability criteria implemented in the instrument control software, based on the stabilization of plate temperatures and heat-flux transducer signals. The instrument employs two calibrated heat-flux transducers located on opposite sides of the specimen. Under steady-state conditions, the effective heat-flux density was determined from the mean of the calibrated sensor readings. Thermal conductivity was evaluated according to Fourier's law using the specimen thickness entered into the HFM Proteus®/SmartMode ver. 9.7 (July 2025) software, the temperature difference, and the heat-flux density. Thermal resistance was calculated as $R = d/\lambda$, where d represents the entered specimen thickness and λ is the reported thermal conductivity. The instrument-recorded plate gap was retained as a separate parameter and is provided in Supplementary Table S1. The specimen edges were left unsealed during the measurements.

Thermal properties were determined using two specimens per variant, each obtained from a different independently manufactured panel, resulting in 12 thermal specimens in total. Thermal conductivity, thermal resistance, and heat flux were determined for each specimen. The upper and lower heat-flux transducers provided measurements of the same specimen and were therefore not treated as independent experimental replicates.

The HFM measurement reports document a heat-flux transducer calibration dated 12 August 2026, using a reference material identified as 1450 D (reference ID 381-4, calibration ID 381-4_10). The calibration was performed at a mean temperature of approximately 10 °C, with recorded calibration factors of 9360.54 and 7665.99 W m^{-2} V^{-1} for the lower and upper heat-flux transducers, respectively. All MDF specimens were measured on 17–18 August 2026 using this calibration record.

2.4. Statistical Analysis

For the mechanical properties, the experimental design consisted of two manufacturing routes (hot and cold pressing) and three nominal panel densities (500, 600, and 700 kg m^{-3}), with three independently manufactured panels per treatment combination. To avoid pseudoreplication, the mean of the five specimen measurements was calculated separately for each panel, and the three independent panel means per variant were used as the experimental observations for inferential statistical analysis. The effects of manufacturing route, nominal panel density, and their interaction on the mechanical properties were evaluated using two-way analysis of variance (ANOVA), with independent panel means as experimental observations. Where applicable, post hoc comparisons were performed using Tukey's honestly significant difference test. Statistical significance was assessed at $p < 0.05$. Thermal properties were analysed separately using two measured specimens per panel variant ($n = 2$). For each specimen, thermal resistance was calculated from the specimen thickness entered into the HFM software and the reported thermal conductivity ($R = d/\lambda$), while heat flux was determined as the mean of the upper and lower heat-flux sensor readings. The arithmetic mean and sample standard deviation were subsequently calculated for each thermal property within each panel variant. Given the limited number of thermal specimens, comparisons between manufacturing routes and nominal density levels were interpreted descriptively rather than as confirmatory statistical tests. All original measurement data are openly available in the RepOD repository (https://doi.org/10.18150/BHYWFJ).

Exploratory relationships between panel structure, thermal behaviour, and mechanical performance were examined using the mean values of the six investigated variants. Given the limited number of observations and the confounding between manufacturing route and density-profile type, these relationships were presented descriptively and were not used to establish predictive models or causal mechanisms. Model assumptions were evaluated by examining residual distributions and the homogeneity of variances.

3. Results

Table 1 summarizes the vertical density-profile descriptors and thermal properties of all investigated panel variants. The results show that panels manufactured using different pressing routes may exhibit substantially different internal density distributions and thermal properties despite having comparable mean densities. The largest difference in thermal conductivity was observed at the nominal density of 600 kg m^{-3}, where the cold-pressed F600 panels exhibited approximately 31.0% lower thermal conductivity than the corresponding hot-pressed U600 panels. The two variants also differed in their surface-to-core density ratios, which were approximately 1.00 and 1.60, respectively. Moreover, F700 exhibited a substantially lower thermal conductivity than U700 despite its slightly higher mean density, indicating that mean density alone was insufficient to explain the observed differences in heat transfer.

Table 1. Summary of vertical density profile characteristics and thermal performance of the investigated fibreboards *.

Parameter	U500	F500	U600	F600	U700	F700
Mean density (kg m^{-3})	502	505	606	602	690	704
Surface density (kg m^{-3})	690	513	811	605	925	721
Core density (kg m^{-3})	412	512	508	612	563	703
Surface/core ratio	1.68	1.00	1.60	0.99	1.64	1.02
Profile CV (%)	19.8	1.8	18.0	3.0	18.8	1.4
HFM input thickness (mm)	9.92	9.92	9.71	9.91	9.22	9.94
λ (W m^{-1} K^{-1})	0.0804 ± 0.0031	0.0713 ± 0.0036	0.1054 ± 0.0033	0.0728 ± 0.0031	0.1199 ± 0.0006	0.0885 ± 0.0001
R (m^2 K W^{-1})	0.1235 ± 0.0049	0.1393 ± 0.0068	0.0921 ± 0.0001	0.1362 ± 0.0059	0.0769 ± 0.0007	0.1123 ± 0.0004
Heat flux (W m^{-2})	145.8 ± 5.8	129.4 ± 6.3	195.4 ± 0.3	132.3 ± 5.7	234.1 ± 2.2	160.2 ± 0.5

* Density-profile descriptors are defined in Section 2.2. Thermal properties are reported as mean ± sample standard deviation (n = 2 specimens per variant). Thickness refers to the value entered into the HFM software. Individual thermal measurement results are provided in Supplementary Table S1 and are also available in the RepOD repository at https://doi.org/10.18150/BHYWFJ.

3.1. Vertical Density Profile

The VDPs of the investigated fibreboards are presented in Figure 1. Two clearly distinct density distributions were obtained. The U-series panels (U500, U600, and U700) exhibited a conventional U-shaped profile characterized by pronounced high-density surface regions and a substantially lower-density core. In contrast, the F-series panels (F500, F600, and F700) exhibited a roughly homogeneous density distribution across most of the panel thickness.

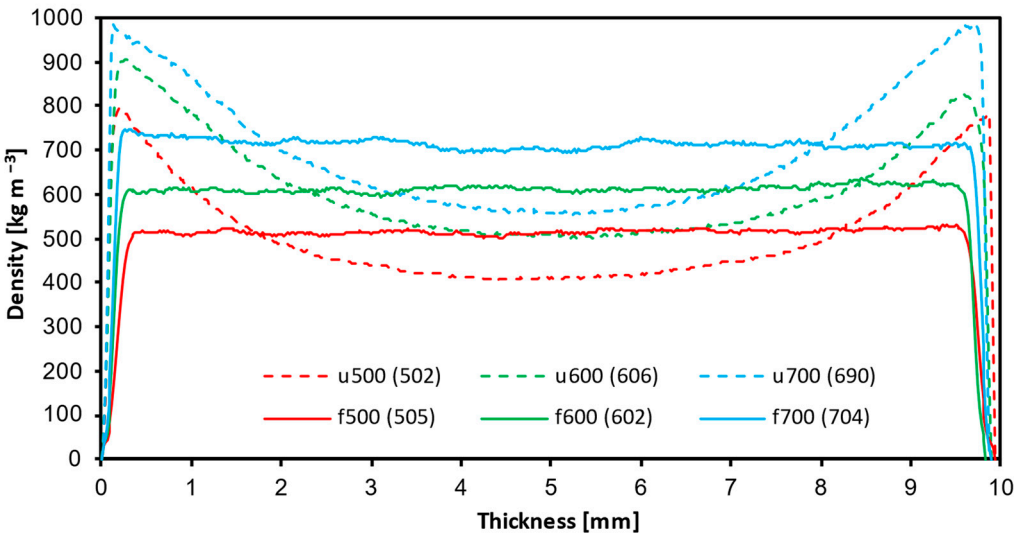

Figure 1. Representative vertical density profiles of the tested panels.

The differences in VDP were achieved while maintaining comparable mean panel densities within the corresponding nominal density groups. The mean densities were 502 and 505 kg m^{-3} for U500 and F500, respectively, 606 and 602 kg m^{-3} for U600 and F600, and 690 and 704 kg m^{-3} for U700 and F700. Thus, the differences between the corresponding U and F panels were only 0.6%, 0.7%, and 2.0% at nominal density levels of 500, 600, and 700 kg m^{-3}, respectively.

The density redistribution through the panel thickness was substantial. The mean surface peak density of the near-surface regions of U500, U600, and U700 was approximately

690, 811, and 925 kg m^{-3}, respectively, whereas the corresponding core densities were approximately 412, 508, and 563 kg m^{-3}. Consequently, the surface-to-core density ratio remained relatively consistent across the U-series, ranging from approximately 1.60 to 1.68.

A fundamentally different distribution was observed for the F-series. The corresponding surface-to-core density ratios were approximately 1.00, 0.99, and 1.02 for F500, F600, and F700, respectively. The density of the central region was approximately 512 kg m^{-3} for F500, 612 kg m^{-3} for F600, and 703 kg m^{-3} for F700. Compared with the corresponding hot-pressed panels, the cold-pressed panels exhibited core densities approximately 24%, 20%, and 25% higher at nominal densities of 500, 600, and 700 kg m^{-3}, respectively.

The magnitude of density variation through the panel thickness further confirmed the structural distinction between the two profile types. The coefficient of variation of density within the principal panel cross-section was approximately 18–20% for the U-series, compared with only approximately 1–3% for the F-series. Thus, panels of almost identical mean density exhibited fundamentally different internal density architectures.

3.2. Thermal Properties

The measured thermal conductivity varied with nominal panel density and differed between the hot-pressed and cold-pressed panel groups, which also exhibited distinct vertical density profiles (Figure 1, Table 1). At each nominal density, the cold-pressed panels exhibited lower thermal conductivity than the corresponding hot-pressed panels.

At the nominal density of 500 kg m^{-3}, the mean thermal conductivity was 0.0804 ± 0.0031 W m^{-1} K^{-1} for U500 and 0.0713 ± 0.0036 W m^{-1} K^{-1} for F500, corresponding to a reduction of 11.3% in the cold-pressed panels. At 600 kg m^{-3}, U600 exhibited $\lambda = 0.1054$ ± 0.0033 W m^{-1} K^{-1}, whereas F600 reached 0.0728 ± 0.0031 W m^{-1} K^{-1}. The difference of 31.0% was the largest observed among the corresponding manufacturing routes. At the highest nominal density, thermal conductivity was 0.1199 ± 0.0006 W m^{-1} K^{-1} for U700 and 0.0885 ± 0.0001 W m^{-1} K^{-1} for F700, representing a reduction of 26.2%.

The thermal measurements were based on two specimens per panel variant ($n = 2$). Therefore, the differences observed between the hot-pressed and cold-pressed panels were evaluated descriptively. Although the measured values indicated differences in thermal conductivity between the two manufacturing routes at all investigated nominal density levels, the limited number of thermal specimens did not provide a sufficiently robust basis for confirmatory statistical inference. Consequently, the reported thermal comparisons should be regarded as preliminary experimental observations requiring further validation with additional independent measurements.

Thermal conductivity increased with nominal density within both manufacturing groups, although the magnitude of this increase differed. Increasing nominal density from 500 to 700 kg m^{-3} increased λ from 0.0804 to 0.1199 W m^{-1} K^{-1} in the hot-pressed series, corresponding to an increase of approximately 49.2%. In the cold-pressed series, λ increased from 0.0713 to 0.0885 W m^{-1} K^{-1}, corresponding to an increase of approximately 24.1%. Thus, within the investigated density range, the increase in thermal conductivity was more pronounced for the hot-pressed panels.

The thickness values entered into the HFM calculations differed among the investigated variants. The mean values were 9.92, 9.71, and 9.22 mm for U500, U600, and U700, respectively, compared with 9.92, 9.91, and 9.94 mm for F500, F600, and F700. The corresponding mean thermal resistances were 0.1235, 0.0921, and 0.0769 m^2 K W^{-1} for the hot-pressed panels, compared with 0.1393, 0.1362, and 0.1123 m^2 K W^{-1} for the cold-pressed panels. Since thermal resistance depends on both specimen thickness and thermal conductivity, these differences should be interpreted with consideration of the specimen-level measurements provided in Supplementary Table S1.

The differences in thermal resistance were reflected in the measured heat flux under comparable temperature gradients. At the nominal density of 600 kg m^{-3}, the mean heat flux was 195.4 ± 0.3 W m^{-2} for U600, compared with 132.3 ± 5.7 W m^{-2} for F600. At 700 kg m^{-3}, the corresponding values were 234.1 ± 2.2 W m^{-2} for U700 and 160.2 ± 0.5 W m^{-2} for F700. These results were obtained under an approximately 18 K temperature difference, and the specimen-level values are provided in Supplementary Table S1.

Figure 2 presents exploratory comparisons between the mean thermal conductivity and selected VDP descriptors for the six panel variants. The U- and F-series occupied distinct regions of the plots, reflecting differences in their manufacturing-induced density distributions and thermal properties. However, the small number of observations and the separation between the two manufacturing groups do not allow independent relationships between VDP descriptors and thermal conductivity to be established. Therefore, these comparisons are presented descriptively, without regression modelling or causal interpretation.

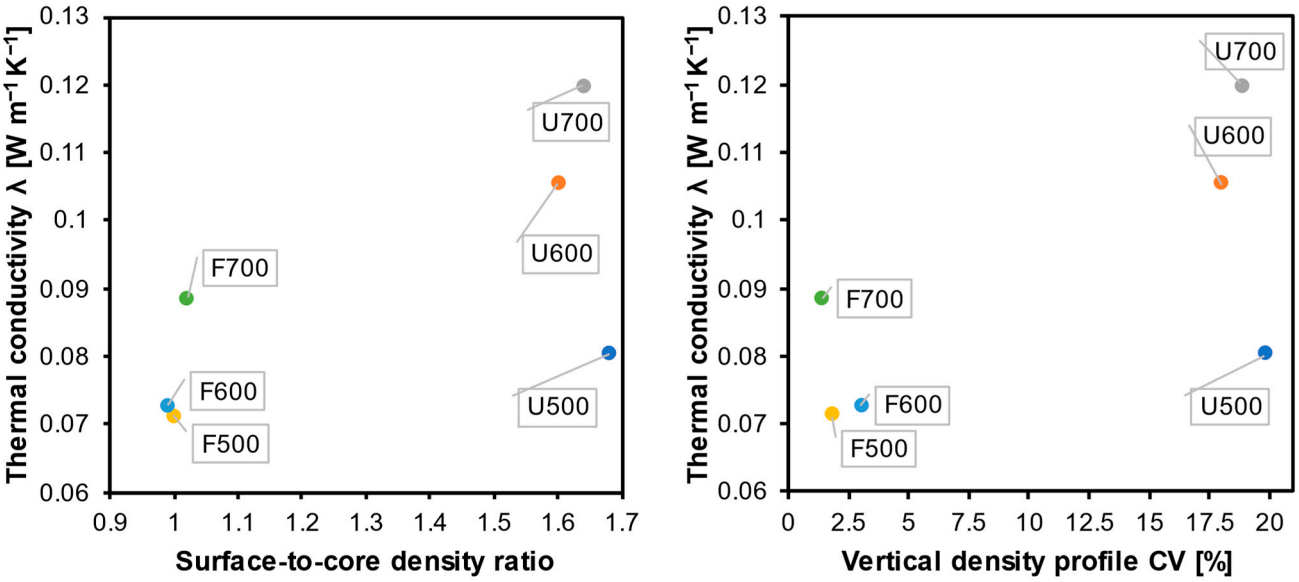

(**a**) (**b**)

Figure 2. Exploratory relationships between thermal conductivity and (**a**) surface-to-core density ratio and (**b**) vertical density profile coefficient of variation. Each point represents the mean value of one panel variant (six variants in total).

In both relationships, the U-profile panels were clearly separated from the F-profile panels in terms of the VDP descriptors. The F-series was characterized by surface-to-core density ratios close to unity and profile CV values of approximately 1–3%, whereas the corresponding values for the U-series were approximately 1.60–1.68 and 18–20%, respectively. The U-series generally exhibited higher thermal conductivity than the F-series. Nevertheless, the dispersion of λ values within the U-series, particularly the relatively low λ of U500 despite its pronounced density profile, indicates that neither the surface-to-core density ratio nor profile CV alone fully explains the variation in thermal conductivity.

3.3. Bending Properties

The bending properties of the investigated panels, presented in Figure 3, differed substantially between the hot-pressed and cold-pressed groups and varied with nominal panel density, particularly within the hot-pressed series. The U-profile panels exhibited substantially higher MOR and MOE than the corresponding F-profile panels at all nominal

density levels. For the U-profile panels, MOR increased from 17.38 ± 0.91 N mm^{-2} for U500 to 20.29 ± 1.06 N mm^{-2} for U600 and 32.19 ± 1.69 N mm^{-2} for U700. The corresponding MOE values increased from 1663 ± 82 N mm^{-2} to 2071 ± 103 N mm^{-2} and 3292 ± 163 N mm^{-2}, respectively. Thus, increasing the nominal density from 500 to 700 kg m^{-3} resulted in an approximately 85% increase in MOR and a 98% increase in MOE. A fundamentally different behaviour was observed for the F-profile panels. MOR remained nearly unchanged between F500 and F600, at 4.54 ± 0.24 N mm^{-2}, and decreased slightly to 3.66 ± 0.19 N mm^{-2} for F700. Similarly, MOE changed only slightly, from 470 ± 23 N mm^{-2} for F500 to 496 ± 25 N mm^{-2} for F600 and 447 ± 22 N mm^{-2} for F700. Consequently, no systematic improvement in bending properties accompanied the increase in nominal density of the F-series.

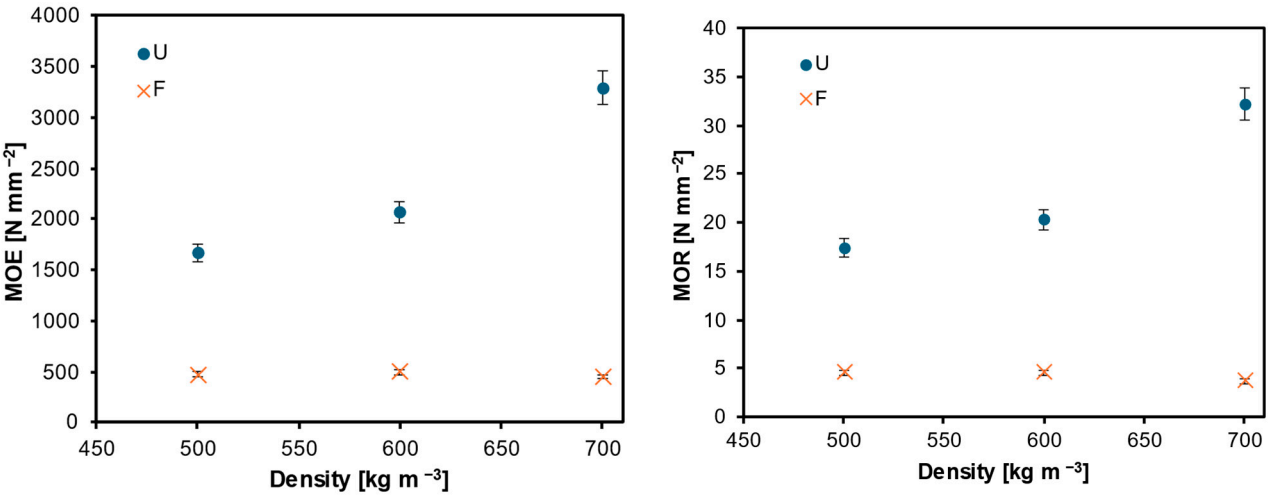

(**a**) (**b**)

Figure 3. Modulus of elasticity (**a**) and modulus of rupture (**b**) of hot-pressed (U) and cold-pressed (F) MDF panels as a function of mean panel density. Symbols represent the mean values of the investigated panel variants, while error bars indicate the standard deviations of three independent panel means (n = 3 per variant).

Comparison of panels at the same nominal density demonstrated substantially higher bending strength and stiffness in the hot-pressed panels than in their cold-pressed counterparts. At 500 kg m^{-3}, MOR and MOE of U500 were approximately 283% and 254% higher, respectively, than those of F500. At 600 kg m^{-3}, the corresponding differences increased to approximately 347% for MOR and 318% for MOE. The largest differences were observed at 700 kg m^{-3}, where U700 exhibited approximately 780% higher MOR and 636% higher MOE than F700.

MOR and MOE exhibited similar trends across the investigated variants, as expected from their related mechanical response during bending. The hot-pressed panels generally showed higher bending strength and stiffness than the corresponding cold-pressed panels. Although these properties appeared to be associated with selected density-profile descriptors, the limited number of variant-level observations does not justify drawing mechanistic conclusions from the calculated correlations.

Across the six investigated variants, higher bending strength and stiffness generally coincided with higher thermal conductivity and heat flux. However, these exploratory associations largely reflected differences between the two manufacturing groups and should not be interpreted as evidence of a direct mechanistic relationship between thermal transport and bending performance.

3.4. Compressive Properties

The compressive stress at 10% strain (σ_{10}) (Table 2) varied with nominal panel density and differed between the hot-pressed and cold-pressed panels, which also exhibited distinct vertical density profiles. The mean σ_{10} values were 0.765 ± 0.078, 0.915 ± 0.094, and 0.897 ± 0.092 N mm^{-2} for U500, U600, and U700, respectively, compared with 0.516 ± 0.053, 0.542 ± 0.056, and 0.895 ± 0.092 N mm^{-2} for F500, F600, and F700, respectively.

Table 2. Compressive stress at 10% strain (σ_{10}) of MDF panels with different vertical density profiles and nominal densities.

Panel Variant	σ_{10} [N mm^{-2}], Mean ± SD	CV (%)
U500	0.765 ± 0.078	10.22
U600	0.915 ± 0.094	10.23
U700	0.897 ± 0.092	10.25
F500	0.516 ± 0.053	10.24
F600	0.542 ± 0.056	10.24
F700	0.895 ± 0.092	10.24

At nominal densities of 500 and 600 kg m^{-3}, the U-profile panels exhibited 48.2% and 68.7% higher σ_{10}, respectively, than the corresponding F-profile panels. In contrast, at 700 kg m^{-3}, the difference between U700 and F700 was negligible (0.897 vs. 0.895 N mm^{-2}).

Two-way ANOVA indicated significant effects of manufacturing route ($p < 0.001$), nominal density ($p < 0.001$), and their interaction ($p < 0.001$) on σ_{10}. Pairwise comparisons indicated differences between the hot-pressed and cold-pressed panels at nominal densities of 500 and 600 kg m^{-3}, whereas no significant difference was observed at 700 kg m^{-3}. These findings suggest that the differences in compression behaviour between the two manufacturing routes depended on nominal panel density.

3.5. Internal Bond Strength

Internal bond strength (Table 3) varied with nominal density and differed between the hot-pressed and cold-pressed panels, which also exhibited distinct vertical density profiles. For the U-profile panels, mean IB increased from 0.493 ± 0.047 N mm^{-2} for U500 to 0.733 ± 0.070 N mm^{-2} for U600 and 0.870 ± 0.083 N mm^{-2} for U700. The corresponding values for the F-profile panels were 0.743 ± 0.071, 0.992 ± 0.095, and 1.220 ± 0.117 N mm^{-2}, respectively.

Table 3. IB of MDF panels with different vertical density profiles and nominal densities.

Panel Variant	IB [N mm^{-2}]	SD [N mm^{-2}]	CV (%)
U500	0.493	0.047	9.53
U600	0.733	0.070	9.55
U700	0.870	0.083	9.54
F500	0.743	0.071	9.56
F600	0.992	0.095	9.58
F700	1.220	0.117	9.59

At each nominal density, the F-profile panels exhibited significantly higher IB than the corresponding U-profile panels. Compared with the U variants, IB was higher by 50.6%, 35.3%, and 40.2% for F500, F600, and F700, respectively ($p < 0.001$ in all pairwise comparisons). The representative photographs in Figure 4 illustrate differences in the observed failure patterns. The U-profile specimens shown exhibited failure near the lower-density central region, whereas the F-profile specimens presented a less clearly localized

failure pattern. These qualitative observations do not provide sufficient evidence for a quantitative assessment of failure-location distributions.



(**a**) (**b**)

Figure 4. Examples of specimen failure during the IB test: (**a**) U-density profile and (**b**) F-density profile.

Two-way ANOVA indicated significant effects of manufacturing route ($p < 0.001$) and nominal density ($p < 0.001$), as well as a significant manufacturing route × density interaction ($p = 0.044$). Internal bond strength increased with nominal density in both panel groups, while the cold-pressed panels exhibited higher resistance to tensile loading perpendicular to the panel plane.

3.6. Relationships Between Structural, Mechanical, and Thermal Properties

Exploratory comparisons of the six variant means indicated that panels exhibiting higher bending strength and stiffness generally also showed higher thermal conductivity and heat flux. These patterns largely reflected differences between the two manufacturing groups. Given the small number of variant-level observations and the confounding between pressing conditions and density-profile type, these correlations were considered descriptive only and were not interpreted as evidence of causal mechanisms.

4. Discussion

4.1. Effect of Manufacturing Conditions on Vertical Density Profile

The substantial differences between the U- and F-series demonstrate that panels of comparable mean density can possess fundamentally different internal density architectures. This is consistent with the established understanding that the vertical density profile of fibreboards is governed by interactions among mat moisture, heat transfer, press-closing conditions, material softening, and time-dependent consolidation.

The U-shaped profiles observed for U500, U600, and U700 are characteristic of conventionally hot-pressed fibreboards. During hot pressing, rapid heating and softening of the surface layers promote their intensive consolidation while the core remains comparatively colder during the initial stage of pressing [15]. Consequently, highly densified outer regions and a lower-density core are formed. Wong et al. [16] similarly demonstrated that mat moisture distribution and pressing strategy strongly affect peak and core densities and can produce either conventional or more homogeneous density profiles.

The nearly constant surface-to-core density ratio of approximately 1.6–1.7 across the U-series indicates that the characteristic profile shape was maintained as mean density

increased. In contrast, ratios close to unity in the F-series confirmed an approximately homogeneous through-thickness density distribution. The cold-pressed panels exhibited core densities approximately 20–25% higher than those of the corresponding hot-pressed panels, reflecting differences in the resulting density distributions associated with the two manufacturing routes. These differences are mechanically relevant because high-density surface layers are particularly effective in bending, whereas internal bond strength is strongly influenced by the lower-density core region. Thus, VDP represents a useful descriptor of the manufacturing-induced internal architecture and may substantially affect panel performance even when mean density remains comparable.

4.2. Effect of Density and Internal Structure on Thermal Properties

Thermal conductivity increased with panel density within both profile groups, consistent with the general behaviour of porous lignocellulosic materials. Increasing density reduces air-filled porosity and increases solid-phase connectivity, thereby facilitating conductive heat transfer. However, the present results show that mean density alone cannot adequately explain the thermal behaviour of the investigated fibreboards. The clearest example is the U600–F600 pair, whose mean densities differed by less than 1% (606 and 602 kg m^{-3}), whereas the cold-pressed F600 panels exhibited approximately 31.0% lower thermal conductivity than U600. Similarly, F700 had a slightly higher mean density than U700 (704 vs. 690 kg m^{-3}), yet its thermal conductivity was approximately 26.2% lower. These results indicate that heat transfer is strongly associated with manufacturing-induced internal structure rather than solely with the amount of solid material per unit volume. Nevertheless, because surface contact resistance was not independently evaluated, the contribution of manufacturing-induced differences in surface characteristics to the measured effective thermal response remains uncertain.

Effective thermal conductivity of fibre-based composites depends on the connectivity of the solid lignocellulosic phase, fibre orientation, pore morphology, fibre-to-fibre contact area, resin distribution, and moisture content. The higher λ of the U-series may therefore be related to the highly consolidated surface regions, which provide more continuous solid-phase conduction pathways. This interpretation is consistent with observations that thermal transport in wood-based panels depends on internal structural organization and cannot be represented adequately by bulk density alone [8,9].

Under the investigated steady-state laboratory conditions, the hot-pressed panels exhibited higher measured thermal conductivity and heat flux, together with lower thermal resistance, than the corresponding cold-pressed panels. However, these observations do not directly demonstrate superior performance in complete flooring assemblies, where operating temperature, moisture content, and interfacial contact conditions may also influence heat transfer.

4.3. Relationship Between Vertical Density Profile and Thermal Conductivity

A simple layered-density model would suggest that the low-density core of a U-profile panel should constitute a thermal bottleneck. For one-dimensional heat transfer perpendicular to the panel plane, individual layers can be considered as thermal resistances arranged in series. Under such an assumption, homogenizing the density profile might be expected to improve heat transfer. The experimental results, however, showed the opposite trend: despite their lower core densities, the hot-pressed panels exhibited higher measured thermal conductivity than their cold-pressed counterparts. Expressed relative to the hot-pressed variants, the thermal conductivity of the cold-pressed panels was approximately 11.3–31.0% lower. This discrepancy indicates that local density alone does not capture the mechanisms governing thermal transport. The high-density surface regions of the U-series may form

highly consolidated fibre networks with more effective solid-phase heat-transfer pathways. At the same time, the manufacturing process may modify fibre orientation, contact geometry, pore-size distribution, and resin distribution. Consequently, the measured VDP should be regarded as a readily quantifiable descriptor of a broader manufacturing-induced microstructure rather than as the sole causal variable determining thermal conductivity.

The exploratory comparisons presented in Figure 2 showed that the two manufacturing groups occupied distinct regions of the plots. However, the limited number of observations and the confounding between manufacturing route and density-profile type prevent the identification of independent relationships between the VDP descriptors and thermal conductivity. Therefore, these observations should be interpreted descriptively rather than as evidence of specific heat-transfer mechanisms.

From an application perspective, these findings suggest that mean panel density alone is insufficient to characterize thermal performance. Future investigations should examine manufacturing routes capable of producing intermediate density profiles under controlled pressing and curing conditions to determine whether a more favourable balance between thermal and mechanical properties can be achieved.

The thermal measurements were conducted under a single set of steady-state conditions using isolated panel specimens. Consequently, the results do not account for temperature-dependent changes in thermal conductivity, variable moisture conditions, or additional thermal resistance associated with interfaces in a complete flooring assembly. The effective thermal response may also be influenced by the interfacial contact resistance between the specimen surfaces and the measuring plates. The substantial differences in surface density between the hot-pressed and cold-pressed panels could be accompanied by differences in surface roughness and real contact area. Consequently, systematic differences in thermal contact resistance may have contributed to the measured U–F differences [4]. However, neither surface roughness nor interfacial thermal resistance was independently determined in the present study, and their contribution cannot be quantified. Investigations of interfacial heat transfer in other porous materials demonstrate the importance of contact conditions, although these findings should be treated as methodological analogues rather than direct evidence for MDF. Further investigations under varied contact pressures and temperatures are therefore recommended.

4.4. Bending Performance of Hot- and Cold-Pressed Panels

The pronounced differences in MOR and MOE between the hot-pressed and cold-pressed panels cannot be attributed exclusively to their vertical density profiles, since the manufacturing conditions also differed substantially. The highly densified surface regions of the hot-pressed panels are consistent with their superior bending performance, as material located further from the neutral axis contributes more strongly to bending stiffness and strength. However, differences in fibre consolidation, adhesive curing, and inter-fibre bonding may also have contributed to the observed mechanical behaviour.

This interpretation agrees with previous studies. Wong et al. [6] reported higher MOR for conventionally profiled fibreboards and increases in MOR and dynamic MOE as peak surface density increased. Xu [17] demonstrated theoretically that increasing outer-layer density enhances MOE, while Zhang and Yu [7] showed that differentiated density profiles can provide markedly higher bending performance than uniform profiles at comparable average density.

The present results follow the same pattern. From U500 to U700, MOR increased by approximately 85% and MOE by approximately 98%, accompanied by an increase in surface density from about 690 to 925 kg m^{-3}. In contrast, increasing the mean density of the F-series did not systematically improve either MOR or MOE. These observations are consistent

with the importance of through-thickness density distribution for bending performance. However, the contribution of local density differences cannot be separated from other manufacturing-related factors, particularly fibre consolidation and adhesive curing.

4.5. Relationship Between Mechanical and Thermal Performance

Across the investigated variants, panels with higher bending strength and stiffness generally also exhibited higher thermal conductivity and heat flux. These exploratory associations may reflect differences in fibre-network connectivity and consolidation; however, they were largely influenced by the differences between the two manufacturing routes. Consequently, they should not be interpreted as evidence of a direct causal relationship between bending performance and thermal transport. Further investigations involving controlled manufacturing conditions are needed to establish the relationships between internal structure and the thermal–mechanical response of MDF panels.

4.6. Compression Behaviour of Hot- and Cold-Pressed Panels

Compression perpendicular to the panel plane was influenced by both nominal density and manufacturing-induced density architecture. At 500 and 600 kg m^{-3}, the U-profile panels exhibited substantially higher σ_{10} than the corresponding F-panels, whereas at approximately 700 kg m^{-3} both profile types reached similar values of about 0.90 N mm^{-2}. The reported manufacturing route × nominal density interaction suggests that the differences in compression behaviour between the two pressing routes varied with nominal density. However, this interaction cannot be interpreted as evidence of an isolated effect of the vertical density profile. This behaviour can be related to differences in through-thickness consolidation. Rathke et al. [18] demonstrated that MDF loaded perpendicular to the panel plane exhibits heterogeneous strain distributions associated with core and transition zones and with local consolidation and curing conditions. The lower σ_{10} values of F500 and F600 may reflect differences in fibre consolidation and bonding associated with the cold-pressing conditions. At the highest nominal density, the two manufacturing routes yielded similar compression resistance. However, the respective contributions of density distribution, adhesive curing, and consolidation conditions could not be separated.

Exploratory comparisons suggested that differences in compression resistance and thermal conductivity were not uniform across the investigated density levels. At approximately 600 kg m^{-3}, the hot-pressed panels exhibited higher compressive stress at 10% strain and higher thermal conductivity than the corresponding cold-pressed panels. In contrast, at approximately 700 kg m^{-3}, the two manufacturing routes produced similar compression resistance despite differences in thermal conductivity. These observations should be interpreted descriptively because the limited number of panel variants does not allow independent relationships between thermal transport and compression behaviour to be established.

4.7. Internal Bond Strength in Relation to Manufacturing-Induced Structure

Internal bond strength increased with nominal density in both panel groups, but the F-profile panels consistently exhibited higher IB than the corresponding U-profile panels. This behaviour is consistent with their higher core densities: approximately 512, 612, and 703 kg m^{-3} for F500, F600, and F700 compared with 412, 508, and 563 kg m^{-3} for the corresponding U-panels. The importance of the core region for IB is well established because tensile failure perpendicular to the panel plane typically occurs within the low-density core or transition regions. Rathke et al. [18] showed that failure and strain localization in MDF are strongly associated with these regions, while Korai [19] demonstrated relationships between minimum/core density and IB. However, both studies also indicate that

bonding quality, adhesive curing, and local structural characteristics contribute to failure behaviour. The qualitative observations of failure during internal bond testing also suggest a potential direction for future numerical investigations. Fracture models incorporating measured vertical density profiles could help determine whether the observed failure locations can be explained by differences in local density distribution or whether additional factors, including adhesive bonding quality and local consolidation, must be considered. Recent cracking-element approaches provide potentially useful methods for simulating quasi-brittle fracture [20,21]. However, applying such models to MDF would require additional experimental characterization and validation, which were beyond the scope of the present study.

The present results likewise show that the bending advantage of the U-profile does not extend to IB. MOR and MOE benefit from high-density material near the surfaces, whereas IB is governed predominantly by the weakest through-thickness region. In the present study, higher core densities were associated with higher IB values, although the contributions of density distribution, adhesive curing, and consolidation conditions could not be separated. This is consistent with the observed failure patterns, which were concentrated near the core in U-panels but less predictable in the approximately homogeneous F-panels. IB showed essentially no linear association with thermal conductivity across the six variants. For example, F600 exhibited higher IB than U600 (0.992 vs. 0.733 N mm^{-2}), while its mean thermal conductivity was substantially lower (0.0728 vs. 0.1054 W m^{-1} K^{-1}). Thus, the structural characteristics governing tensile integrity perpendicular to the panel plane are not identical to those governing heat transfer across the entire thickness.

Overall, the two investigated manufacturing routes produced panels with different combinations of thermal and mechanical properties. The hot-pressed panels exhibited higher thermal conductivity and bending performance, together with higher compression resistance at the lower and intermediate nominal densities, whereas the cold-pressed panels showed higher internal bond strength. These observations demonstrate the need to consider manufacturing conditions and the resulting internal structure together when developing MDF panels for applications requiring specific thermal and mechanical characteristics.

A major limitation of the present study is that the two panel series were manufactured under substantially different pressing conditions. These differences may have affected not only the resulting density profiles but also fibre consolidation, adhesive curing, and inter-fibre bonding. In particular, the relatively low MOR values of the cold-pressed panels (3.66–4.54 N mm^{-2}) may partly reflect differences in consolidation and curing rather than the approximately flat density profile alone. Since the adhesive curing state was not independently characterized by DSC, FTIR, or other suitable techniques, its contribution cannot be quantified. Consequently, the observed differences should be interpreted as combined manufacturing-route and structural effects rather than evidence of an isolated influence of VDP.

5. Conclusions

This study demonstrated that MDF panels manufactured by hot and cold pressing exhibited distinct vertical density profiles and thermal–mechanical properties despite having comparable mean densities. Hot-pressed panels with conventional U-shaped profiles showed higher thermal conductivity, lower thermal resistance, and substantially better bending strength and stiffness. In contrast, cold-pressed panels with approximately flat profiles exhibited higher internal bond strength. Compression behaviour depended on nominal density, with the differences between the two panel types diminishing at approximately 700 kg m^{-3}. These findings highlight the trade-offs between thermal and mechanical performance associated with different manufacturing-induced internal structures.

The observed differences cannot be attributed exclusively to vertical density profiles because the manufacturing routes also differed in pressing conditions. Furthermore, thermal characterization was limited to two specimens per variant under a single set of steady-state conditions. Further research should therefore focus on controlled manufacturing conditions, intermediate density profiles, and additional thermal measurements, including validation in complete flooring assemblies intended for underfloor heating.

Supplementary Materials: The dataset supporting the conclusions of this article is available as Supplementary Dataset S1 at https://doi.org/10.18150/BHYWFJ.

Author Contributions: S.K.: State of the art, formal analysis, investigation, data curation, writing—original draft, writing—review and editing, and resources; G.K.: Conceptualization, methodology, investigation, validation, writing—original draft, writing—review and editing, funding acquisition, project administration, and resources. All authors have read and agreed to the published version of the manuscript.

Funding: This research received no external funding.

Institutional Review Board Statement: Not applicable.

Informed Consent Statement: Not applicable.

Data Availability Statement: The experimental data supporting the findings of this study are openly available in the RepOD research data repository at https://doi.org/10.18150/BHYWFJ (created and accessed on 3 September 2026).

Acknowledgments: This research was conducted with the support of the Student Furniture Scientific Group (Koło Naukowe Meblarstwa), Faculty of Wood Technology, Warsaw University of Life Sciences—SGGW, Warsaw, Poland. The authors gratefully acknowledge NETZSCH Instrumenty Sp. z o.o. (Kraków, Poland) and Henryk Orszulak, Sales Engineer, for providing the NETZSCH instrument used for the thermal measurements in this study.

Conflicts of Interest: The authors declare no conflicts of interest.

Abbreviations

The following abbreviations are used in this manuscript:

MOR	Modulus of Rupture
MOE	Modulus of Elasticity
IB	Internal Bond
λ	Thermal Conductivity Coefficient
R	Thermal Resistance
VDP	Vertical Density Profile
σ_{10}	Compressive stress at 10% strain
CV	Coefficient of Variation
RH	Relative Humidity

References

1. Seo, J.; Jeon, J.; Lee, J.H.; Kim, S. Thermal Performance Analysis According to Wood Flooring Structure for Energy Conservation in Radiant Floor Heating Systems. *Energy Build.* **2011**, *43*, 2039–2042. [CrossRef]
2. Jara, E.Á.R.; Ruiz-Pardo, Á.; García, M.C.; Ríos, J.A.T. Effect of Wood Properties and Building Construction on Thermal Performance of Radiant Floor Heating Worldwide. *Appl. Sci.* **2022**, *12*, 5427. [CrossRef]
3. Ruiz-Pardo, Á.; Jara, E.Á.R.; García, M.C.; Ríos, J.A.T. Influence of Wood Properties and Building Construction on Energy Demand, Thermal Comfort and Start-Up Lag Time of Radiant Floor Heating Systems. *Appl. Sci.* **2022**, *12*, 2335. [CrossRef]
4. Tang, K.; Wen, M.; Zhang, Y.; Ge, X. Experimental Study on the Measurement of Interfacial Thermal Contact Resistance of Layered Porous Materials. *Case Stud. Therm. Eng.* **2025**, *76*, 107363. [CrossRef]
5. Minhas, A.H.; Ullah, N.; Riaz, A.A.; Siddiqi, M.U.R.; Abualnaja, K.M.; Althubeiti, K.; Muhammad, R. Experimental Investigation of Vertical Density Profile of Medium Density Fiberboard in Hot Press. *Appl. Sci.* **2021**, *11*, 10769. [CrossRef]

6. Wong, E.D.; Zhang, M.; Wang, Q.; Han, G.; Kawai, S. Formation of the Density Profile and Its Effects on the Properties of Fiberboard. *J. Wood Sci.* **2000**, *46*, 202–209. [CrossRef]
7. Zhang, Y.; Yu, Z. Effects of Vertical Density Profiles on Bending Properties of Fiberboard with a "Bowl-Shaped" Vertical Density Profile. *For. Prod. J.* **2011**, *61*, 510–516. [CrossRef]
8. Czajkowski, Ł.; Olek, W.; Weres, J.; Guzenda, R. Thermal Properties of Wood-Based Panels: Thermal Conductivity Identification with Inverse Modeling. *Eur. J. Wood Wood Prod.* **2016**, *74*, 577–584. [CrossRef]
9. Czajkowski, Ł.; Olek, W.; Weres, J.; Guzenda, R. Thermal Properties of Wood-Based Panels: Specific Heat Determination. *Wood Sci. Technol.* **2016**, *50*, 537–545. [CrossRef]
10. Imken, A.A.P.; Kraft, R.; Mai, C. Production and Characterisation of Wood-Fibre Insulation Boards (WFIB) from Hardwood Fibres and Fibre Blends. *Wood Mater. Sci. Eng.* **2022**, *17*, 802–808. [CrossRef]
11. *EN 310*; Wood-Based Panels—Determination of Modulus of Elasticity in Bending and of Bending Strength. European Committee for Standardization: Brussels, Belgium, 1993.
12. *EN 319*; Particleboards and Fiberboards—Determination of Tensile Strength Perpendicular to the Plane of the Board. European Committee for Standardization: Brussels, Belgium, 1993.
13. *EN ISO 29469*; Thermal Insulating Products for Building Applications—Determination of Compression Behaviour. European Committee for Standardization: Brussels, Belgium, 2022.
14. *EN 12664*; Thermal Performance of Building Materials and Products—Determination of Thermal Resistance by Means of Guarded Hot Plate and Heat Flow Meter Methods—Dry and Moist Products of Medium and Low Thermal Resistance. European Committee for Standardization: Brussels, Belgium, 2002.
15. Li, K. On Determining Density and Specific Heat of New Zealand Medium Density Fibreboard. *Procedia Eng.* **2013**, *62*, 769–777. [CrossRef]
16. Wong, E.D.; Zhang, M.; Wang, Q.; Kawai, S. Formation of the Density Profile and Its Effects on the Properties of Particleboard. *Wood Sci. Technol.* **1999**, *33*, 327–340. [CrossRef]
17. Xu, W. Influence of Vertical Density Distribution on Bending Modulus of Elasticity of Wood Composite Panels: A Theoretical Consideration. *Wood Fiber Sci.* **1999**, *31*, 277–282.
18. Rathke, J.; Sinn, G.; Konnerth, J.; Müller, U. Strain Measurements within Fiber Boards. Part I: Inhomogeneous Strain Distribution within Medium Density Fiberboards (MDF) Loaded Perpendicularly to the Plane of the Board. *Materials* **2012**, *5*, 1115–1124. [CrossRef] [PubMed]
19. Korai, H. Difficulty of Internal Bond Prediction of Particleboard Using the Density Profile. *J. Wood Sci.* **2021**, *67*, 64. [CrossRef]
20. Zhang, Y.; Li, J.; Wen, M. Cracking Elements with Sequential Linear Analysis: An Efficient Event-Driven Numerical Framework for Quasi-Brittle Fracture. *Finite Elem. Anal. Des.* **2026**, *262*, 104649. [CrossRef]
21. Zhang, Y.; Huang, J.; Yuan, Y.; Mang, H.A. Cracking Elements Method with a Dissipation-Based Arc-Length Approach. *Finite Elem. Anal. Des.* **2021**, *195*, 103573. [CrossRef]

Disclaimer/Publisher's Note: The statements, opinions and data contained in all publications are solely those of the individual author(s) and contributor(s) and not of MDPI and/or the editor(s). MDPI and/or the editor(s) disclaim responsibility for any injury to people or property resulting from any ideas, methods, instructions or products referred to in the content.